PNC-TN9410 87-161

Key Technological Design Study of a Large LMFBR (Ⅱ)

System Dynamics Analysis for Mitigating ATWS Consequences of a 1000MWe Looq-Type LMFBR

November, 1987

OARAI ENGINEERING CENTER
POWER REACTOR AND NUCLEAR FUEL DEVELOPMENT CORPORATION

複製又はこの資料の入手については，下記にお問い合わせください。
〒311-13　茨城県東茨城郡大洗町成田町4002
動力炉・核燃料開発事業団
大洗工学センター　システム開発推進部・技術管理室

Enquires about copyright and reproduction should be addressed to: Technology Management Section O-arai Engineering Center, Power Reactor and Nuclear Fuel Development Corporation 4002 Narita-cho, O-arai-machi, Higashi-Ibaraki, Ibaraki-ken, 311-13, Japan

動力炉・核燃料開発事業団（Power Reactor and Nuclear Fuel Development Corporation）

PNC-TN9410 87-161
１９８７年１１月

Key Technological Design Study of a Large LMFBR (Ⅱ)

System Dynamics Analysis for Mitigating ATWS Consequences of a 1000MWe Looq-Type LMFBR

山口勝久*

要　　旨

1000MWe 級ループ型高速増殖炉を対象に，炉停止失敗事故を想定した場合の事象推移を解析し，高速増殖炉の有する固有の事故緩和能力を評価した。

解析では，従来から仮想炉心崩壊事故の解析に用いられてきた反応度フィールドバック以外に，制御棒延長管の軸方向熱膨張による炉心への制御棒挿入効果，炉心支持板の径方向熱膨張による炉心全体の膨張効果を考慮できるようにした。炉設計では，チムニー型炉上部機構を考え，主循環ポンプ流量半減時間，制御棒待機位置をパラメータと扱った。

流量喪失事故は，流量半減時間が４０秒以上となるように設計対応するか，１０秒以上で制御棒待機位置を250㎜炉心に挿入した位置になるようにすることにより，事象推移を緩和し，冷却材最高温度を飽和温度以下に抑えることができる。除熱系機能喪失事故は，約１００℃下廻る温度レベルで流量喪失事故と類似した事象推移をたどる。反応度挿入事故は，６０¢の反応度を持つ制御棒が１～３¢／Ｓで挿入される設計条件では，最高ナトリウム温度が６５０℃以下，燃料溶融割合が２５％以下の現行基準以内に納まる。

＊　動力炉・核燃料開発事業団，大洗工学センター，安全工学部，原子炉工学室

PNC-TN9410 87-161
November.1987

Key Technological Design Study of a Large LMFBR (Ⅱ)

System Dynamics Analysis for Mitigating ATWS Consequences of a 1000MWe Looq-Type LMFBR

K. Yamaguchi*

ABSTRACT

A system dynamics analysis was applied to a 1000 MWe loop-type liquid-metal fast breeder reactor (LMFBR) to examine influence of possible innovative reactor designs on mitigating consequences of anticipated transients without scram (ATWS). The analysis included all the reactivity feedbacks having been employed in current analyses of hypothetical core disruptive accidents (HCDAs). In addition, the present analysis stressed inherent responses of the reactor system by including structural reactivity feedbacks due to axial expansion of control rod driveline (CRD) and radial expansion of reactor core driven by the expansion of the core support plate (CSP). An upper-core flow chimney was considered to make the CRD expansion feedback effective. The flow coastdown rate of the primary pump and the initial position of the control rod (CR) were treated as parameters. ATWS initiators examined were unprotected loss-of-flow (ULOF), loss-of-heat-sink (ULOHS) and transient overpower (UTOP).

The ULOF accident was mitigated and peak sodium temperature was suppressed below boiling point by using the primary pump having a 40 s halving time of flow coastdown. The halving time could be shortened to 10 s by assuming that the CR was initially inserted into the active core by about 250 mm. The CRD expansion feedback controlled the earlier transient, and the CSP expansion feedback became dominant in the latter phase. The ULOHS consequence was completely enveloped in that of ULOF accident. The sodium temperatures in the primary system became lower than the ULOF case by about 100 °C. The UTOP accident conceivable from the current plant design, i.e., the reactivity insertion of 60 ¢ with the rate of 1 to 3 ¢/s, suppressed sodium temperatures and fuel melt fractions below 650 °C and 25 %, respectively.

* Reactor Engineering Section, Safety Engineering Division, O-arai Engineering Center, Power Reactor and Nuclear Fuel Development Corporation.

MONENCLATURES

c_p : specific heat [kJ/kg°C]
d : thickness [m]
F_{PM} : pony moter flow [%]
h : heat transfer coefficient [W/m^2°C]
k : thermal conductivity [W/m°C]
L : loop length [m]
l_p : prompt neutron life time [s]
P : pressure [MPa]
S : surface area [m^2]
T : temperature [°C]
t : time [s], and thickness [m]
V : volume [m^3]
W : mass flow rate [kg/m^{2}s]
β : delayed neutron precursor fraction [-], and linear expansion coefficient [1/m°C]
Δz_{CR} : initial control rod insertion length [m]
ρ : density [kg/m^3], and reactivity [Dollar]
$\tau_{1/2}$: halving time of flow coastdown [s]

INTRODUCTION

The current emphasis in the design of liquid-metal fast breeder reactors (LMFBRs) is to develop inherently safe reactor systems to preclude hypothetical core disruptive accidents (HCDAs) while maintaining low capital costs. Key to the successful prevention of core disruption in unprotected overpower and under-cooling accidents, i.e., anticipated transients without scram (ATWS), is the design provision for inherent, passive mechanisms which respond to the upset condition and act to restore the balance between reactor power production and system cooling. In the unprotected loss-of-flow (ULOF), loss-of-heat-sink (ULOHS) and transient overpower (UTOP) accidents, the upset leads to an increase in coolant temperatures in the reactor system. Negative reactivity feedbacks caused by this coolant temperature increase can be effective in limiting accident consequences. Two such mechanisms can be provided by the net insertion of the control rods (CRs) into active core caused by differential thermal expansion of the control rod drivelines (CRDs), and by radial core expansion driven by thermal expansion of the core support plate (CSP).

The ULOF and other ATWS tests were performed in the Rapsodie, EBR-II and FFTF reactors[1],[2],[3]. The implication from these tests was that the CRD elongation and radial core expansion provided the overall nagative reactivity feedbacks which could shutdown the reactor power during the coolant heatup. The ULOF evaluations by Chang et al.[2],[4],[5] indicate that these two feedback mechanisms become effective in different time phases: During the first phase, which extends over the initial one to two hundred seconds of the accident, the CRD elongation contributes primarily to shutting the fission power down to an acceptable power level so that boiling and fuel damage are precluded. After this initial period, the CSP becomes hot enough to enhance radial core expansion. By this expansion, the reactor power continues to decrease until the decay power level. The major concern left thereafter involves assuring that acceptable temperatures are maintained by the decay heat removal system (DHRS) and the main heat transport system (MHTS).

The small reactors tested have negative coolant density coefficients. This limits the large positive reactivity insertion as the sodium temperature increases. On the contrast, the coolant density coefficient changes positive and the Doppler coefficient becomes very large as the core size increases. Therefore, the passive reactor shutdown capability available to small reactors does not necessarily hold in the large reactor case. The enhancement of the passive shutdown mechanisms is required especially in the field of large LMFBR developments. Yet, no systematic studies have been carried out on coupled thermal-hydraulic and nuclear-kinetic evolution for such cases.

The purpose of this paper is to investigate the influence of several significant innovative design features on mitigating consequences of ATWS. A numerous sensitivity analysis was performed on a typical 1000 MWe loop-type LMFBR, for which an optimization approach of innovative design features is not known from the current state of the art. The ATWS initiators examined were ULOF, ULOHS and UTOP, while our efforts were directed with emphasis to the ULOF accident analysis.

REACTOR DESCRIPTION

The reactor plant cited in the present study is not a specified but a typical loop-type LMFBR designed to operate at a thermal power output of 2600 MW and a net electrical power output of about 1000 MW. A schematic representation of the plant is given in Fig. 1. The plant has four MHTSs. Each system consists of a primary loop, a secondary loop and a water/steam loop. The primary sodium at 360 °C is driven by the pump with a rated flow rate of 1.31×10^7 kg/h. It enters the common cold plenum of the reactor vessel, goes up through reactor core being heated, and reaches the common hot plenum where it mixes with the bulk sodium and becomes 500 °C. Leaving the reactor vessel, it moves to the intermediate heat exchanger (IHX) and is cooled again to 360 °C. The IHX transfers the 650 MW energy generated in the reactor to the secondary sodium system and ultimately to the steam generator (SG) and the turbogenerator. The rated flow rate and the hot-leg/cold-leg sodium temperatures of the secondary circuit are 1.14×10^7 kg/h and 470/310 °C, respectively. The secondary circuit has an intermediate reactor auxiliary cooling system (IRACS) which is devised as a DHRS.

The reactor vessel is 8 m in diameter and 15 m in height, containing a core of 6 m in diameter and 4 m in height. The reactor core is composed of 355 Oxide-fueled driver assemblies, 24 CRs, 150 radial blankets, 505 radial shields, and 149 in-vessel spent fuel storage (IVS) assemblies. The active core is 1 m in height and is subdivided into inner and outer cores whose diameters are 2.7 and 3.4 m, respectively. The length of each axial blanket is 0.3 m. The fuel assembly spaced triangularly with a radial pitch of 165.8 mm contains a 271-pin, wire-spacer bundle having a 0.35 MPa pressure drop at the nominal operating condition. The diameter of fuel pin is 7.5 mm and the maximum heat flux is 43 kW/m.

ANALYTICAL MODEL

A flow network analysis code of the reactor primary system was used for the present study. The code modeled flow mixing in the plenum, heat transport along the flow path and heat transfer between the sodium and the structures. It has a

capability of treating transient thermal-hydraulics with a fine node scheme.

Figure 2 shows the flow network model applied to the reactor vessel. It is assumed that the 90 % rated flow entering the reactor vessel moves straight to high pressure plenum located just below the CSP, and that the residual 10 % of primary flow mixes with the bulk sodium at the lowest cold pool and joins thereafter to the main flow at the high pressure plenum. The high pressure plenum supplies the fuel assembly flow, while some part of the sodium flow branches into the low pressure plenum and then separates into radial blankets and neutron shields depending on the pressure drop characteristics of these assemblies and structures.

As pointed out by Sienicki[6], the hot sodium introduced into the upper plenum during the flow coastdown rises buoyantly toward the top of the plenum, thereby providing the thermal expansion of the CRD. To enhance this heatup-induced elongation of the driveline, an innovative design of an upper core flow chimney was considered in the flow network model. The chimney locates above the CR and its neighboring six fuel assemblies, and encompasses each CRD in the upper plenum. The effect of the chimney on the flow distribution is, however, sensitive to design details. Therefore, it is assumed from the geometrical configuration of the chimney that the 40 % of sodium flow from the core passes through the devised chimnies.

The thermal-hydraulics of the reactor core is represented by the single-pin model usually used in one-dimensional safety analysis codes. Figure 3 illustrates the axial and radial node divisions. The core is represented by seven channels: inner core, outer core, CR, fuel neighboring with CR, radial blanket, radial shield, and hottest channel having maximum power-to-flow ratio in steady state. The IVS assembly was neglected. All of these assemblies are tightly supported by the CSP, thereby moving radially together with the CSP which expands radially during thermal upsets. The radial bowing of those assemblies and the inter-assembly flow and heat redistribution, both of which may be very important inherent safety features[5],[7], are not taken into account: Fox et al.[7] descrived that the assembly bowing introduced an effective negative feedback for a small, free flowering reactor core, whereas Gouriou et al.[8] reported that the feedback effect became unexpectedly small enough to be neglected for a large, pad-spacing reactor core like that treated here. On the other hand, Coffield et al.[5] analyzed that the steady state hot-spot factor (by which the thermal-hydraulic conditions of the hottest channel were given) could be decreased approximately in half by the inter-assembly flow and heat redistribution, which had a significant benefit with regard to suppressing the peak sodium temperature in the hottest channel. From these discussions, we can conclude that the present model would lead to conservative results. Furthermore, the calculation is simplified conservatively by neglecting the axial displacement of the active core, which might be caused by axial expansions of core support structures, hexcans and lower region of the pin itself.

Neutronics is represented by point kinetics where the prompt neutron life time and delayed neutron precursor fractions are given in Table 1. The reactivity coefficients are evaluated as shown in Table 2, while some of them might have large uncertainties. Therefore, the Doppler and sodium density reactivity coefficients are treated as having 30 and 50 % errors, respectively. The reactivity caused by the fuel contraction is hidden by the opposite, negative feedback of fuel stack expansion by assuming that the fuel pellets swell as they

are irradiated and stick into the cladding so that the fuel stack expands in contact with the cladding[1]. The fuel contraction effect is separately examined in the parametric study.

ULOF ANALYSIS

Typical ULOF consequence

The calculational conditions of the ULOF consequences are listed in Table 3. Among 33 cases calculated, the last 4 cases belong to the preliminary examination where all of the inherent safety features are neglected and the number of loops required to preclude sodium boiling at the hottest channel is seeked. The flow coastdown rate is fixed to be $\tau_{1/2}$ = 5.5 s in these calculations. The results are shown in Fig. 4. A glance at the figure implies that a simultaneous failure of two primary pumps is a borderline case to prevent the ULOF accident from going to an HCDA without any inherent safety features.

Taking into account the aforementioned inherent safety features and innovative designs, a total loss of pumping power accident coupled with a failure of the reactor shutdown system was analyzed in the residual 29 cases. Figure 5 shows the result of the reference (REF) case. This is the typical, coupled thermal-hydraulic and nuclear-kinetic evolution of the ULOF accident which involves inherently shutting the core down to decay heat so that boiling is precluded.

The flow coastdown leads to a steep increase in the sodium temperature at the hottest channel as well as at the other assemblies. Figure 5(a) shows that the initial temperature increase is so fast that the peak temperature overshoot of about 350 °C is reached in 200 s after flow coastdown. We can see from Fig. 5(b) that the temperatures at the upper plenum also increase with the same trend, although there are some transport delays of hot sodium from core to upper plenum. The heatup of the rising sodium within the chimney follows promptly the heatup of CRD (T45), introducing the negative reactivity feedback after about 25 s into the transient. Figures 5(c) and 5(d) show the reactivity balance and the power and flow histories. At first, the Doppler reactivity is negative, because the sodium temperature increase provides an increase in fuel temperatures due to the short-term heat accumulation within the fuel pins. However, the subsequent power reduction caused by the CRD and the other negative reactivity feedbacks leads to the decrease in fuel temperatures, thereby making the Doppler feedback positive. Over the initial heatup phase of 200 s, the net reactivity is kept around -10 ¢ level to shut the reactor core down to around 20 % rated power level. The CRD elongation feedback is a major nagative reactivity component during this initial phase. The fuel pellet displacement in contact with the expanding cladding also introduces prompt negative reactivity feedback. On the other hand, the steel (clad and hexcan) expansion reactivity is positive but is negligibly small.

After 200 s when the temperature peak is reached in the reactor core, the CSP expansion feedback becomes a major factor to reduce the reactor power (the time period when the temperature peak has been attained and the CSP feedback becomes dominant is termed the latter phase in this paper to distinguish it from the initial or earlier phase where the CRD feedback is superior than the CSP feedback). Figure 5(b) revealed that the sodium temperature increased rather rapidly at the CSP (T20). This was partly because the REF calculation assumed

the instantaneous thermal isolation of the primary circuit at the IHX. Therefore, the cold-leg sodium was replaced by the hot-leg sodium having an initial temperature of 500 °C in about 30 s, i.e., the time required for the hot-leg sodium to circulate throughout the cold-leg piping. Another reason was that the small effective heat capacity of the sodium in the lower plenum prevented the coming sodium from being overcooled in the lower plenum. Nevertheless, the CSP temperature (T108) do increase very slowly due to the large heat capacity of the CSP. The slow heatup of the CSP and the associated growth of negative feedback by CSP expansion continue over 1200 s. The reactor is completely shutdown to decay power level in 500 s after flow coastdown. A new quasi-stationary condition will be sustained after 1200 s at a temperature level of around 750 °C. The operator's recovery action to cool the primary sodium by the IRACS is expected at this stage.

The comparison between the present analytical predictions and those of Super-Phenix (SPX) by Gouriou et al.[8] suggests several interesting features relevant to the inherent safety of large LMFBRs. The exit temperatures of the hottest channels behave similarly in both cases because the flow coastdown rates of both plants are nearly equal. The plant analyzed here has a smaller sodium inventory and the chimney structure around the CRD. They can force the CRD and CSP expansion feedbacks more effective than in PSX. Still, the temperatures in the primary system become higher in shorter time. Therefore, we can conclude that our efforts should be concentrated on enhancing further more the prompt, negative reactivity feedbacks in the design consideration of the loop-type LMFBR so that the reactor can be shutdown as fast as possible.

Effects of cooling conditions

The effect of the flow coastdown rate on the resultant ULOF consequences was estimated in the CD1 ($\tau_{1/2}$ = 20 s) through CD4 ($\tau_{1/2}$ = 120 s) cases under complete CR withdrawal conditions, and in the BCD1 ($\tau_{1/2}$ = 10 s) through BCD3 ($\tau_{1/2}$ = 30 s) cases under partial CR insertion (Δz_{CR} = 250 mm) conditions. In addition, the initial CR position was altered systematically under fixed flow coastdown rate ($\tau_{1/2}$ = 60 s) condition in BP1 (Δz_{CR} = 500 mm) through BP3 (Δz_{CR} = 100 mm) cases. The results of these survey calculations are summarized in Figs. 6(a) and 6(b), where the peak sodium temperatures reached at the hottest channel are plotted against flow coastdown rate and CR position. These case studies suggested two important features:

(1) The primary flow coastdown rate gives significant effects on peak sodium temperature, but a little bit on mixed mean sodium temperatures. This indicates that the released thermal energy over the transient time remains almost unchanged, and that the extended flow coastdown contributes to suppress local temperature overshoot during the initial transient phase.

(2) The initial CR insertion into the active core gives drastic effects on both peak sodium temperature and bulk sodium temperatures. This shows that the released energy becomes small as the CR is inserted partially beforehand.

Using the results of REF and BCD2 cases both of which were occasioned to attain the same peak sodium temperature level under different combinations of flow coastdown rate and CR position, an intercomparison was made in Table 4 concerning the power-to-flow mismatching, reactivity balance, and temperature distribution at the time when the peak temperature was reached in each case. The mismatching of power-to-flow ratio per unit time lapse is four times larger in

BCD2 case than in REF case. Accordingly, the response of the temperatures at the wide part of the primary system delays in BCD2 case to a great extent. The reactivity balance is influenced by this difference in transient thermal-hydraulics: The prompt feedback terms, e.g., Doppler and CRD feedbacks, become relatively important as the flow coastdown rate becomes fast. Therefore, again from Fig. 6(a), it is worth notice that a selection of the pump having $\tau_{1/2}$ = 10 to 15 s flow coastdown rate requires the partial CR insertion of 100 to 250 mm into active core to enhance the CRD prompt feedback for mitigating the ULOF consequence.

In the fast flow coastdown cases (e.g., $10 \leq \tau_{1/2} \leq 15$ s), the pony moter flow level becomes of importance than in the slow flow coastdown cases (e.g., $40 \leq \tau_{1/2} \leq 60$ s) for cooling the overshot hot channels and mixing the sodium in the primary system. This is shown in Fig. 6(C). The pony moter was switched on at 380, 220 and 140 s after flow coastdown in order of REF, PM1 and PM2 cases ($\tau_{1/2}$ = 60 s), and at 50 and 25 s in BCD1 and BPM1 cases ($\tau_{1/2}$ = 10 s), respectively. Whether or not the pony moter switching time is earlier than the time when the sodium temperature reaches the peak value in the absence of the pony moter determines the importance of the pony moter operation. For the fast transient (BCD1 and BPM1) cases, the pony moter operations can apparently terminate the rising trends of sodium temperatures in the core to yield peaks in 5 to 10 s after pony moter operations. Once the pony moter begins to contribute to suppressing the temperature peaking, the reactivity balance becomes altered a little: The CRD expansion feedback becomes smaller during the earlier phase. The resultant smaller, nagative net reactivity stays the reactor power rather high. In contrast, the CSP expansion feedback becomes more enhanced during the latter phase. Accordingly, the reactor power begins to fall rapidly at the midway of the transient.

CRD and CSP expansion feedbacks

The REF case assumed that the CRD was made of a stainless steel pipe of 90 mm in diameter and 2 mm in thickness, inside of which was there stagnant sodium. The structure of this CRD was modified in the CR1 (doubled CRD expansion) and CR2 (doubled CRD heat capacity) cases. The doubling of the CRD elongation suppressed the peak sodium temperature by about 50 °C. In contrast, the doubling of the CRD heat capacity introduced no impact into the consequence. The implication of these results is that the chimney should be degigned as long as possible (so that the higher temperature sodium can be collected with sufficient mass flow rate even if the flow coastdown rate is fast and the longer part of the CRD can be bathed in the hot sodium collected), and that a tough pipe can be chosen for the CRD when the chimney suffices such a high performance.

The heatup rate of the CSP can be approximated by

$$\dot{T} = hS\Delta T/c_{p\rho}V$$

where, V/S is a volume-to-surface ratio of the CSP, $c_{p\rho}$ is a heat capacity, ΔT is a temperature difference between coolant and structure, and h is a heat transfer coefficient which is given by

$$h \approx 2k/d$$

where, k is a thermal conductivity and d is a thickness. Therefore, $\dot{T}$ depends on S/Vd and ΔT.

The effect of the geometrical configuration of CSP, i.e., the factor S/Vd, on the ATWS mitigation was examined by comparing the results of REF (nominal volume) and GP1 (×1/2 volume) cases for slow transients ($\tau_{1/2}$ = 60 s), and by BCD1 (nominal volume) and BGP1 (×1/2 volume) cases for fast transients ($\tau_{1/2}$ = 10 s). The comparison indicated that the reduction in the heat capacity decreased the peak sodium temperature by about 40 °C for the slow transient cases, but by only a few degree C for the fast transient cases. On the other hand, the effect of the factor ΔT was examined from two points: One is the influence of mixing volume in the lower plenum which suppresses the heatup rate of the sweeping sodium over the CSP as the mixing volume increases. The other is the influence of primary loop length which delays the arrival of hot sodium as the loop becomes long. The result of GP3 case showed that the full consideration of the plenum volume for the mixing raised the peak sodium temperature by only 10 °C though the transient was slow enough to make the CSP expansion feedback most powerfull. Similar results were obtained in the PL1 and PL2 cases, viz. the peak sodium temperatures increased by about 5 and 20 °C for 25 and 100 m longer piping conditions, respectively.

The conservatism of the REF case prediction was checked because the assumption that the instantaneous thermal isolation of the primary system from the secondary one at the IHX might lead to an over-estimation of the core inlet temperature which could make the CSP negative feedback carelessly enhanced. The survey calculation of HR3 (IHX heat transfer is considered) case revealed that the REF case gave us lower peak temperature at the hottest channel by about 40 °C. However, it was confirmed that the trend of the thermal-hydraulic and nuclear-kinetic consequence was not distorted by this assumption. Therefore, it was concluded that the peak temperature under-estimation like this was negligible in optimizing the plant design. In contrast, when the secondary circuit was treated to operate continuously with hypothetical low temperature of 310 °C at the IHX inlet (HR1 and HR2 cases), the sodium peak temperature ultimately exceeded beyond boiling point. The same situation occurred when the CSP expansion feedback was neglected in the slow transient (GP2 case).

These survey calculations on the CSP expansion feedback led to the following conclusion: The reduction in the CSP heat capacity becomes important only when the transient is so slow that the reactor power is still high for a long time, and that the effective, negative CSP expansion feedback becomes very important to shut the power down to an acceptable level. In such a case, the operating condition of the secondary system becomes influential to the CSP expansion feedback.

Optimization approach

The results of the parametric survey shown above is summarized in Fig. 7, where key factors for mitigating the ULOF consequences are picked up together with the ULOF accident scenario generalized by the present study. The most important design consideration is the development of the chimney type upper-core structure (UCS) shown in Fig. 2 by which hot sodium can be collected around the CRD. The initial position of the CR, as well as the flow coastdown rate, has also very important meaning for optimizing the plant design. The pony moter specification becomes important when the flow coastdown rate is left fast by adopting the design that the CR is usually inserted into the active core by several hundred millimeters.

In general, the reactivity coefficients have uncertainties. Especially,

the transient fuel behavior has a possibility of introducing both negative and positive feedbacks depending on whether or not the irradiated fuel pellets stick to cladding on different points on their circumference along fuel column height. The present calculations assumed the perfect fuel stick behavior. However, since we could not have sufficient confidence in this assumption, an additional calculation (FC1 case) was carried out neglecting the fuel stick behavior. The result indicated that the peak sodium temperature increased by about 40 °C under the slow transient condition analyzed, and that the magnitude of this excess temperature might become large as the flow coastdown rate became fast, for which further detailed investigation was required.

The uncertainties in the reactivity coefficents are of primary concern in the safety analyses. The Doppler and sodium density feedbacks were, therefore, multiplied by factors 1.3 and 1.5 respectively in the RE1 (1.3×Doppler), RE2 (1.5×sodium) and RE3 (1.3×Doppler + 1.5×sodium) cases, and the ULOF consequences followed were compared with that of REF case. The comparison showed that the excess temperatures over nominal value were 15, 55 and 65 °C for RE1 through RE3 cases. The uncertainty in the sodium density coefficient is most sensitive to the resultant consequence. Therefore, much efforts should be concentrated on diminishing this error, while it is beyond the scope of the present study.

ULOHS ANALYSIS

The instantaneous thermal isolation of the primary system from the secondary one at the IHX was assumed again as well as in the calculations of many cases of the ULOF analysis, while the primary pump was left untripped in the present ULOHS analysis.

The predicted ULOHS consequence is shown in Fig. 8, where the other conditions were equal to those of ULOF/REF case. A comparison between the temperature histories shown in Figs. 5 and 8 reveals the similarity between the ULOF and ULOHS consequences. Since the primary system is thermally isolated, the thermal-hydraulic and nuclear-kinetic transient begins with the arrival of the hot-leg sodium of 500°C at the core inlet. The sweep of this coolant out of the core could raise the core exit temperature by 140°C, i.e., the initial temperature difference between cold-leg and hot-leg, if the reactor power did not decrease. The similar transients occur in the succeeded sodium circulations, although the magnitude of the temperature increase becomes small as the power decreases.

The heatup of sodium first enhances the CRD expansion feedback and then the CSP expansion feedback, because the large CSP heat capacity delays the heatup of CSP. The introduced negative reactivity lowers the reactor power with the almost same trend as predicted for the ULOF consequence. The CSP expansion feedback becomes dominant after elapsing a sufficient time which is a little shorter than the ULOF case. The reduction in the reactor power suppresses the increasing tendency of the sodium temperature, leading to the attainment of the temperature peak of about 785 °C at 230 s after loss of heat sink. This peak temperature level is lower than that of ULOF case by about 100 °C. The power reduction diminishes the temperature rise at the core region. Accordingly, the sodium temperatures in the primary system begin to converge into the same level until 300 s by releasing the stored energy to the structures.

As described above, the coupled thermal-hydraulic and nuclear-kinetic evolution of the ULOHS accident was completely enveloped in that of ULOF accident. No additional and special design consideration is, therefore, required to prevent the ULOHS accident from going into an HCDA.

UTOP ANALYSIS

The UTOP accident can be represented by an erroneous withdrawal of a certain control rod from the reactor core. Therefore, a ramp insertion of the external reactivity was assumed in the present study within the restricted scope of the reactivity insertion rate from 1 to 5 ¢/s and the maximum reactivity from 60 to 100 ¢ (the calculational conditions are listed in Table 5). These values of parameters were selected from the current CR design that the reactivity worth of one CR is around 60 ¢ and that the CR drive machine has a performance of withdrawing the rod with the rate of 1 to 3 ¢/s.

Figure 9 shows the predicted histories of reactor power, flow and reactivity balance during the reference UTOP accident (REF case). The insertion of the external reactivity causes the increases in the reactor power and the fuel temperature, introducing the negative Doppler feedback which can cancel out nearly all of the external reactivity insertion. As a result, the net reactivity is maintained around 4 ¢ level over the ramp reactivity insertion period, and falls to 0 after the external reactivity reaches the maximum level. Due to the reactivity unbalance, the power level reaches a new steady level which is 1.3 to 1.4 times as high as the initial power. The power change brought about an excess sodium temperature rise of only 75°C. In the hottest channel, the fuel temperature exceeded beyond fuel melting point at the axially peaked power position along about 200 mm height. The cross-sectional fraction of the molten region in the fuel pellet was about 7 %. However, in the inner and outer core assemblies, the peak fuel temperatures were below melting point and were about 2600 and 2200°C, respectively.

The parametric survey calculations concerning the reactivity insertion rate, i.e., TD2 (3 ¢/s) and TD3 (5 ¢/s) cases, revealed that the consequences are insensitive to this parameter because the Doppler feedback responses fast enough to cancel out the external reactivity insertion in question. However, the increase in the maximum reactivity to 100 ¢ level (TR2 case) resulted in a fuel failure which was defined by the fuel melt fraction over 25 % at the hottest channel: The power level was raised by the factor 1.6 to 1.7, the peak sodium temperature became 670 °C, and the fuel melt fractions reached 60 and 7 % in the hottest channel and inner core assemblies, respectively. The borderline condition to prevent the UTOP consequence from going to the fuel failure was interporated as 70 ¢ reactivity insertion.

When the CRs were initially inserted into the active core by 250 mm (TD1 case), the power level did not rise to the level as high as that of REF case under the same UTOP accident condition. When the CRD and CSP expansion feedbacks were neglected (TR1 case), the fuel melt fraction increased to 10 % level. In any case, the effects of these innovative factors are very small. The most important requirements for the plant design against UTOP are to restrict the maximum reactivity worth of any CR within 60 ¢ and to devise a reliable interlock logic circuit for contradicting the sequential CR withdrawals, for which we will be able to prepare with no difficulties.

CONCLUSION

A system dynamics analysis was applied to a 1000 MWe loop-type LMFBR to examine influence of possible innovative designs on mitigating consequences of ATWS. The analysis included all the reactivity feedbacks employed in the current analysis of HCDA. In addition, the present analysis stressed inherent responses of the reactor system by including structural reactivity feedbacks due to axial expansion of CRD and radial expansion of CSP. The analytical results were summarized and the following conclusions were drawn:

(1) It was confirmed that a simultaneous failure of two primary pumps was a borderline case to prevent the ULOF accident from going to an HCDA without any innovative design. A chimney type UCS was considered in the analysis to introduce powerful CRD expansion feedback. With this innovative design, a total loss of pumping power accident was analyzed. The ULOF accident was mitigated and sodium temperatures were suppressed below boiling point by using the primary pump having a 40 s halving time of flow coastdown. The halving time could be shortened to 10 s by assuming that the CR was initially inserted into the active core by about 250 mm. It was found out that the CRD expansion feedback controlled the earlier thermal upset, and that the CSP expansion feedback dominated the long-term transient. The bulk sodium temperature became close to 800 °C level at 1200 s, when a recovery action was assumed to terminate the ULOF consequence.

(2) The ULOHS consequence was completely enveloped in that of the ULOF accident, and the sodium temperature level was lowered by about 100 °C.

(3) The typical UTOP accident conceivable from the current plant design, i.e., the reactivity insertion of 60 ¢ with the CRD withdrawing velocity of 1 to 3 ¢/s, suppressed sodium temperatures and fuel melt fractions below 650 °C and 25 %, respectively. The innovative design considerations for the CRD and CSP were rather insensitive to the consequences obtained.

ACKNOWLEDGMENTS

The authors would like to thank Messrs. K. Satoh, H. Ieda, N. Nonaka, and F. Kasahara for their suggestions and advice. This study was conducted under the sponsorship of Plant Engineering Section of PNC. The authors are indebted to the project manager, Y. Taniyama.

REFERENCES

(1) C. Essig et al., "Dynamic Behaviour of Rapsodie in Exceptional Transient Experiments," International Topical Meeting on Fast Reactor Safety, CONF-850410, Knoxville, TN, Apr. 1985.
(2) L. K. Chang et al., "An Experimental and Analytical Investigation of Unprotected Loss-of-Flow Events in EBR-II," Trans. Am. Nucl. Soc., Vol 50, pp. 350-351, San Francisco, CA, Nov. 1985.
(3) A. Padilla et al., "The Role of FFTF in Assessing Structural Feedbacks and Inherent Safety of LMR's," International Topical Meeting on Fast Reactor Safety, CONF-850410, Knoxville, TN, Apr. 1985.
(4) L. K. Chang and D. Mohr, "The Effect of Primary Pump Coastdown Characteristics on Unprotected Loss-of-Flow Transients in EBR-II," Second

Specialists' Meeting on Decay Heat Removal and Natural Convection in LMFBRs, Long Island, NY, Apr. 1985.

(5) R. D. Coffield et al., "Thermal-Hydraulic and Nuclear Kinetic Considerations Involved with LMR Inherent Safety," Second International Topical Meeting on Nuclear Power Plant Thermal Hydraulics and Operations, Tokyo, Japan, Apr. 1986.

(6) J. J. Sienicki, "Open Upper Plenum LOF Thermal Hydraulics and Inherent Control Rod Insertion," Trans. Am. Nucl. Soc., Vol 52, pp. 503-504, Reno, NE, June 1986.

(7) J. N. Fox, E. L. Gluekler and N. W. Brown, "Safety Features of a Small Modular Liquid-Metal Reactor," Trans. Am. Nucl. Soc., Vol 50, pp. 336-337, San Francisco, CA, Nov. 1985.

(8) A. Gouriou et al., "The Dynamic Behavior of the Super-Phenix Reactor under Unprotected Transient," International Topical Meeting on Fast Reactor Safety, Lyon, France, July 1982.

Table 1 Neutron kinetics parameters

Parameter		Value
Effective delayed neutron precursor fractions (β_{eff})		3.7×10^{-3}
Six-group components:	β_1	7.5×10^{-5}
	β_2	7.7×10^{-4}
	β_3	6.7×10^{-4}
	β_4	1.4×10^{-3}
	β_5	6.4×10^{-4}
	β_6	1.8×10^{-4}
Prompt neutron lifetime (l_p)		0.4 μs

Table 2 Temperature coefficients of the reactivities

Reactivity coefficient		Value	
Doppler	(Tdk/dT)	-8.3×10^{-3}	
Sodium	(Δk/k/°C)	$+7.3\times10^{-6}$	
Fuel	(Δk/k/°C)	-2.6×10^{-6}	
Steel	(Δk/k/°C)	$+4.1\times10^{-6}$	
CRD	(Δk/k)	-8.1×10^{-2}	*
CSP	(Δk/k/°C)	-1.2×10^{-5}	

* This value is multiplied by the relative reactivity given from the relative reactivity vs. CR position curve.

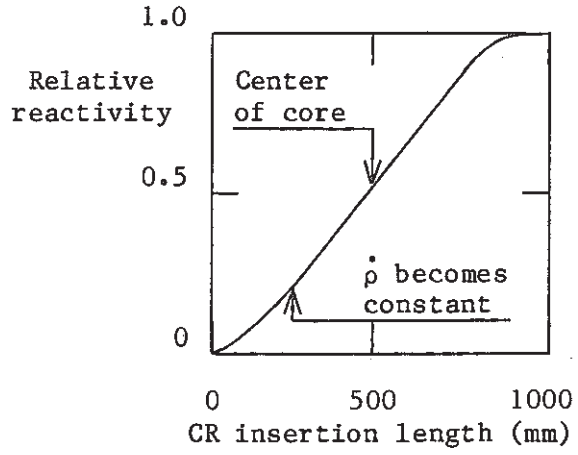

Table 3 Calculational conditions of the ULOF consequences

Category	Case ID	Calculational conditions
Reference	REF	4-loop pump trip, $\tau_{1/2}$ = 60 s, F_{PM} = 9 %, Δz_{CR} = 0 mm, fuel stick assumption, primary loop is thermally isolated.
Pump coastdown rate	CD1	$\tau_{1/2}$ = 20 s
	CD2	25
	CD3	40
	CD4	120
	BCD1	Δz_{CR} = 250 mm, $\tau_{1/2}$ = 10 s
	BCD2	15
	BCD3	30
CRD structure	CR1	$2\times\beta_{CRD}$ (Doubled CRD expansion)
	CR2	$2\times t_{CRD}$ (Doubled CRD heat capacity)
CR position	BP1	Δz_{CR} = 500 mm
	BP2	250
	BP3	100
CSP structure	GP1	$0.5\times V_{CSP}$ (Halved CSP heat capacity)
	GP2	$\infty\times V_{CSP}$ (No CSP expansion)
	GP3	coolant full mixing in the lower plenum
	BGP1	Δz_{CR} = 250 mm, $\tau_{1/2}$ = 10 s, $0.5\times V_{CSP}$
Loop length	PL1	L = 85 m (+ 25 m)
	PL2	160 (+100 m)
Pony moter flow level	PM1	F_{PM} = 20 %
	PM2	30
	BPM1	Δz_{CR} = 250 mm, $\tau_{1/2}$ = 10 s, F_{PM} = 30 %
Fuel stick	FC1	No stick
Reactivity coefficient	RE1	1.3×Doppler
	RE2	1.5×Sodium
	RE3	1.3×Doppler + 1.5×Sodium
Heat removal of primary system	HR1	$T^2_{IHX,in}$ = 310 °C, $\tau^2_{1/2}$ = 5 s, F^2_{PM} = 20 %
	HR2	10
	HR3	310 for $0 \leq t \leq 100$ s
		650 for $t > 100$ s
Pump trip loop	PT1	1-loop pump trip without inherent safety
	PT2	2
	PT3	3
	PT4	4

Table 4 Comparison of power-to-flow mismatching, reactivity balance and temperature distribution

Item	REF case $\tau_{1/2}$ = 60 s Δz_{CR} = 0 mm	BCD2 case $\tau_{1/2}$ = 15 s Δz_{CR} = 250 mm
peak sodium temperature	875 °C (at t = 220 s)	870 °C (at t = 100 s)
Power	17 %	20 %
Flow	18 %	10 %
Reactivity balance		
• Doppler	0.26 Dollar	0.63 Dollar
• Sodium	0.32	0.18
• Fuel	-0.10	-0.54
• CRD	-0.32	-0.93
• CSP	-0.30	-0.10
• Total	-0.14	-0.28
Temperature distribution		
• CRD (T35, T45)	837, 837 °C	782, 782 °C
• Outlet (T121, T141)	802, 728	653, 561
• Inlet (T135, T155)	740, 517	495, 394
• CSP (T20, T108)	709, 457	482, 393

Table 5 Calculational conditions of the UTOP consequences

Category	Case ID	Calculational conditions
Reference	REF	$\dot{\rho}$ = 1 ¢/s, $\Delta\rho_{max}$ = 60 ¢ Other conditions are equal to those of ULOF/REF case
Reactivity insertion rate	TD2	$\dot{\rho}$ = 3 ¢/s
	TD3	5
Maximum reactivity	TR2	$\Delta\rho_{max}$ = 100 ¢
CR position	TD1	Δz_{CR} = 250 mm
Without CRD and CSP feedbacks	TR1	$0\times\beta_{CRD}$, $\infty\times V_{CSP}$ (No CRD and CSP expansions)

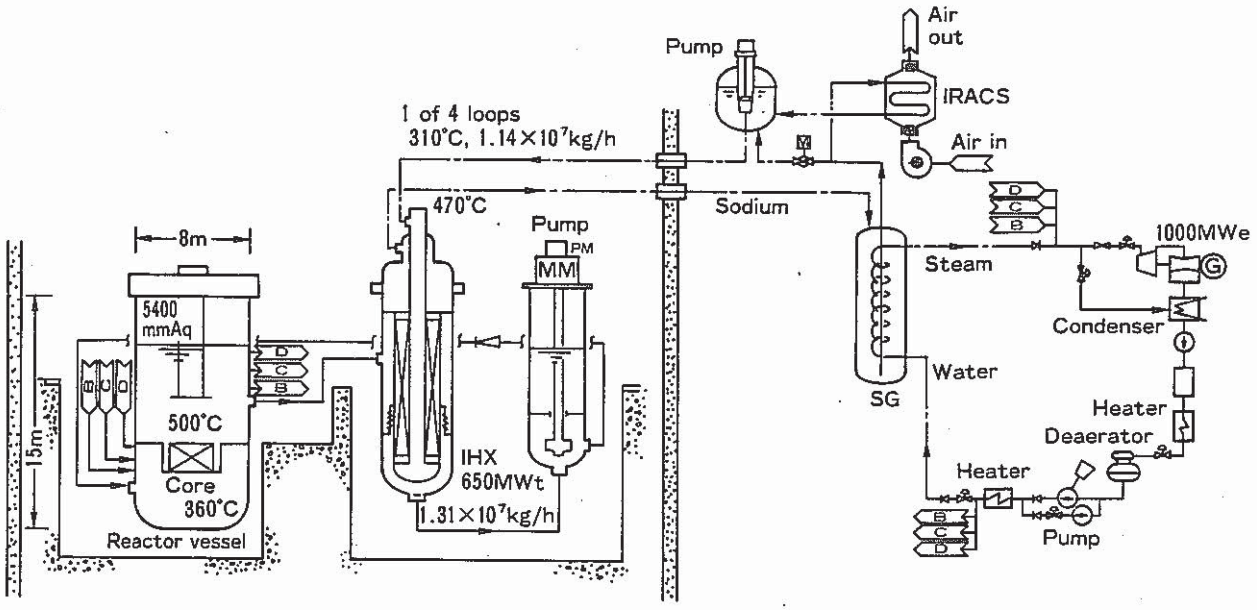

Fig. 1 Schematic flow diagram of a 1000 MWe loop-type LMFBR

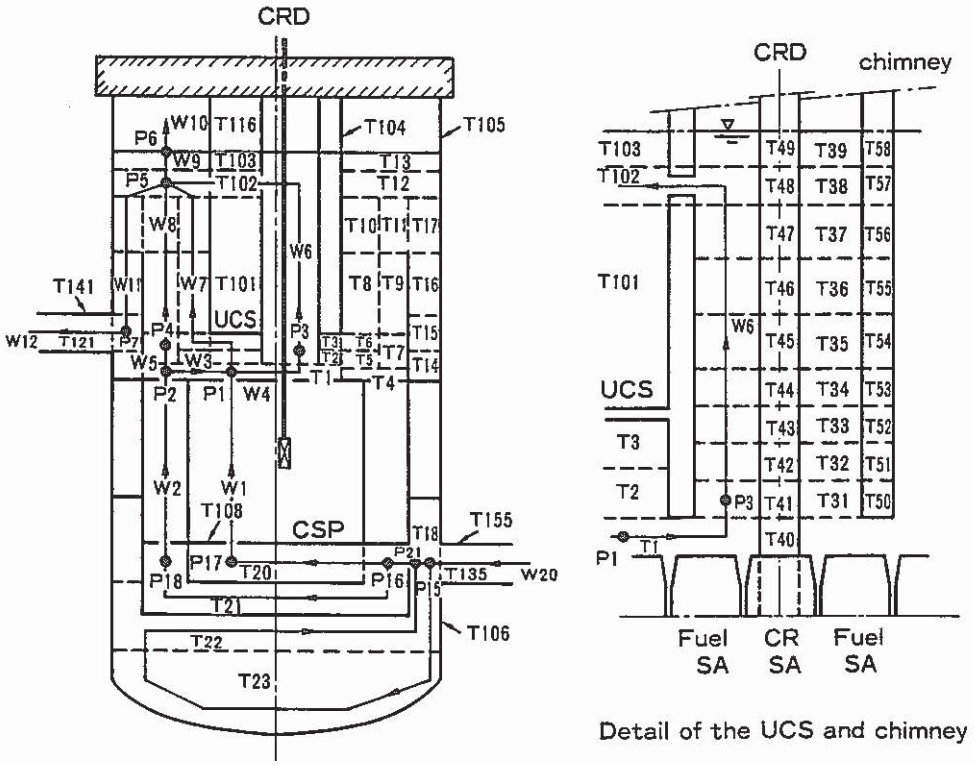

Fig. 2 Flow network model of the reactor vessel

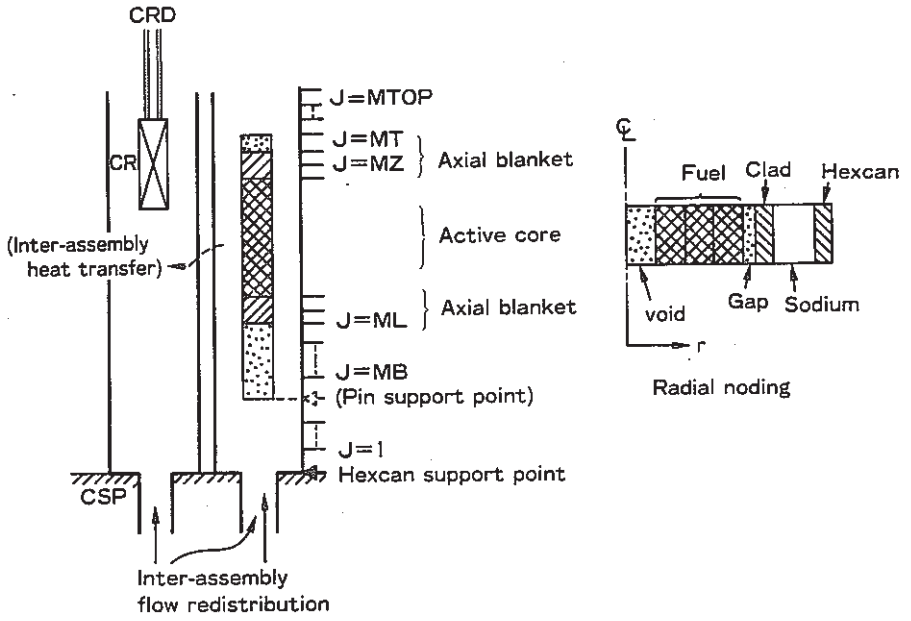

Fig. 3 Single-pin, multi-channel model

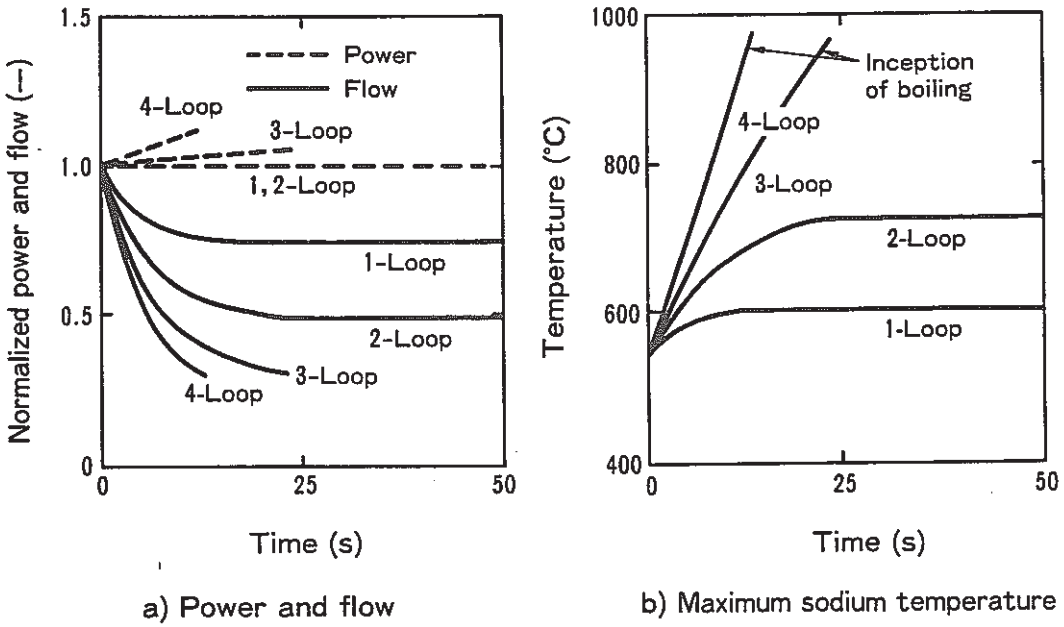

Fig. 4 Effect of trip loops on the ULOF consequences without inherent safety features

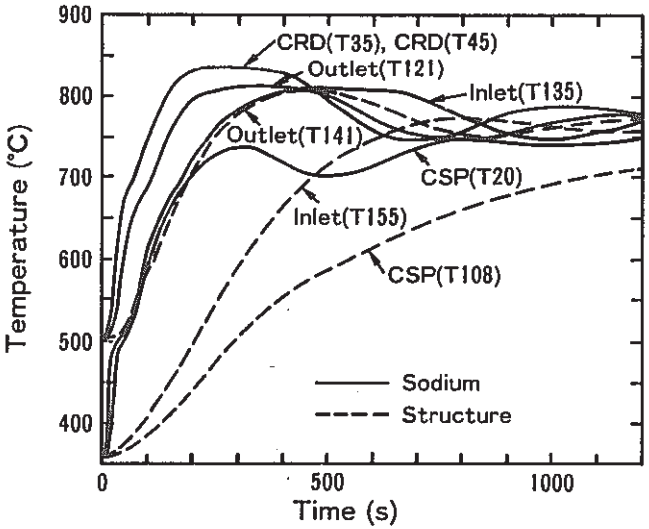

b) Sodium and structure temperatures at the reactor vessel

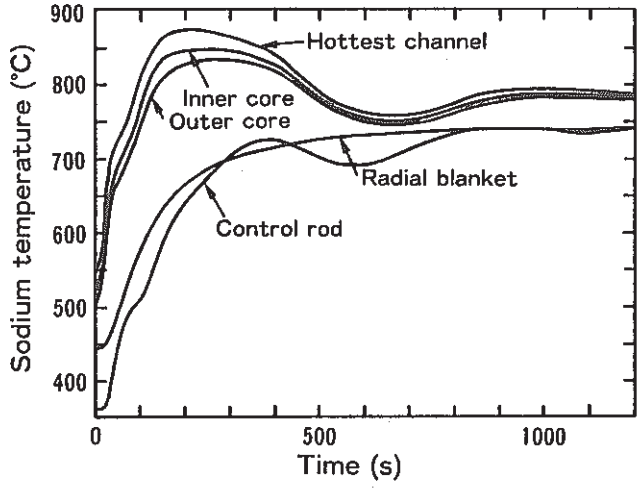

a) Sodium temperatures at the assembly exits

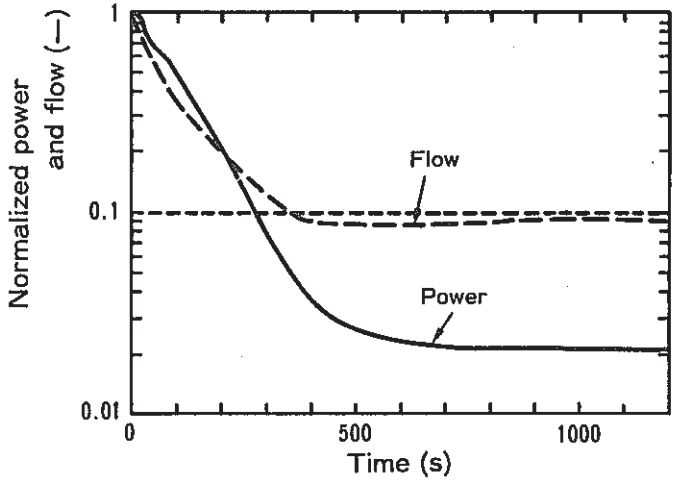

d) Total power and flow

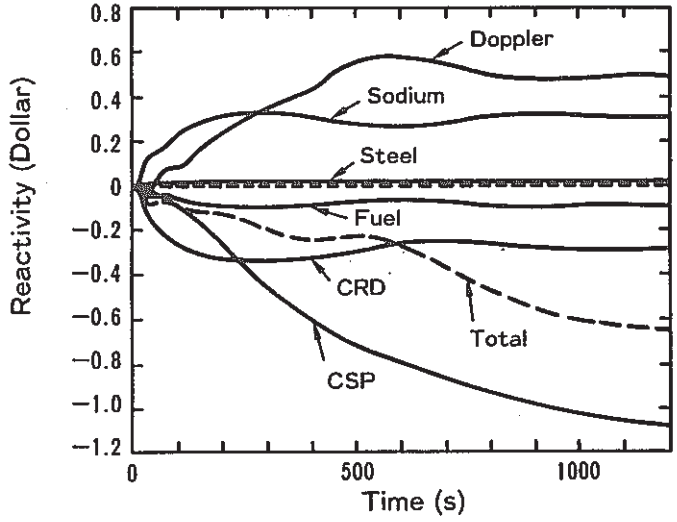

c) Reactivity balance

Fig. 5 Predicted ULOF consequence considering inherent safety features

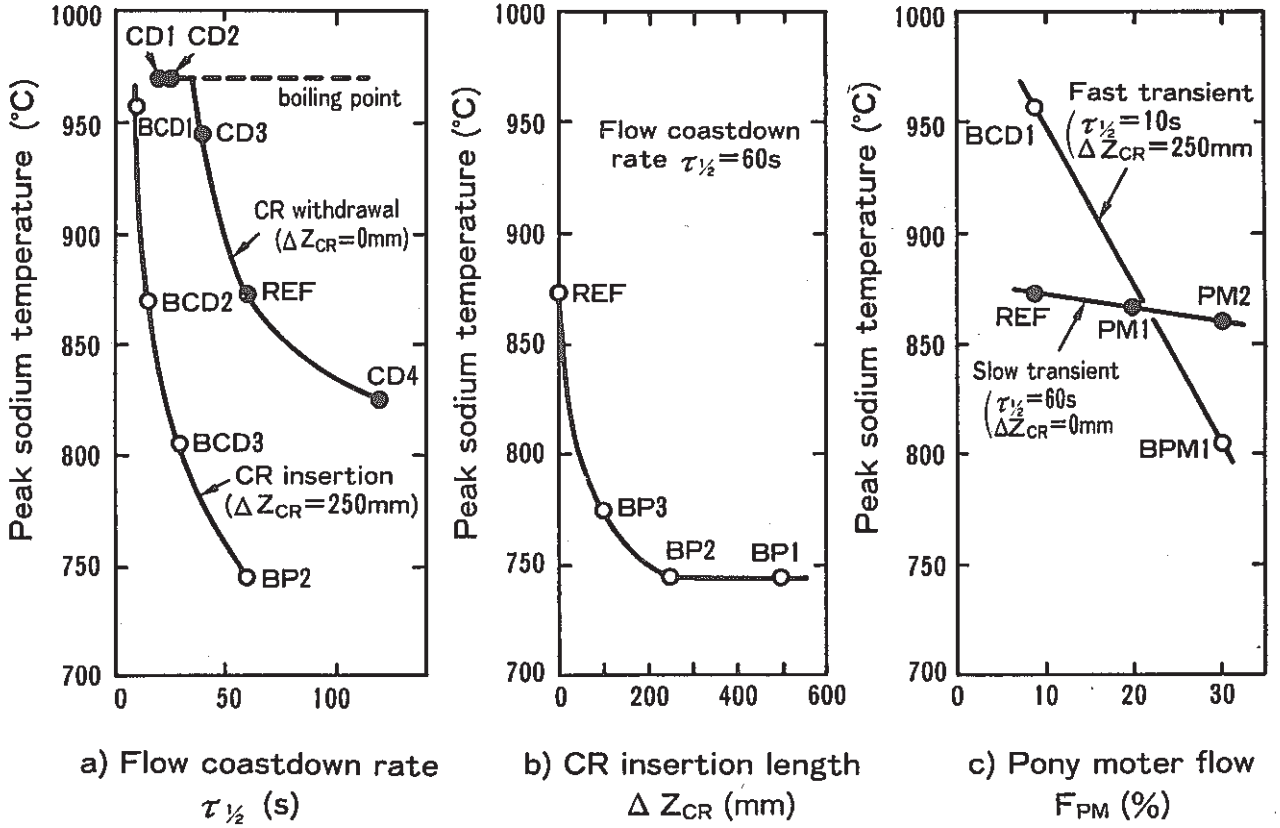

Fig. 6 Effects of flow coastdown rate, CR insertion and pony moter flow on the ULOF consequences

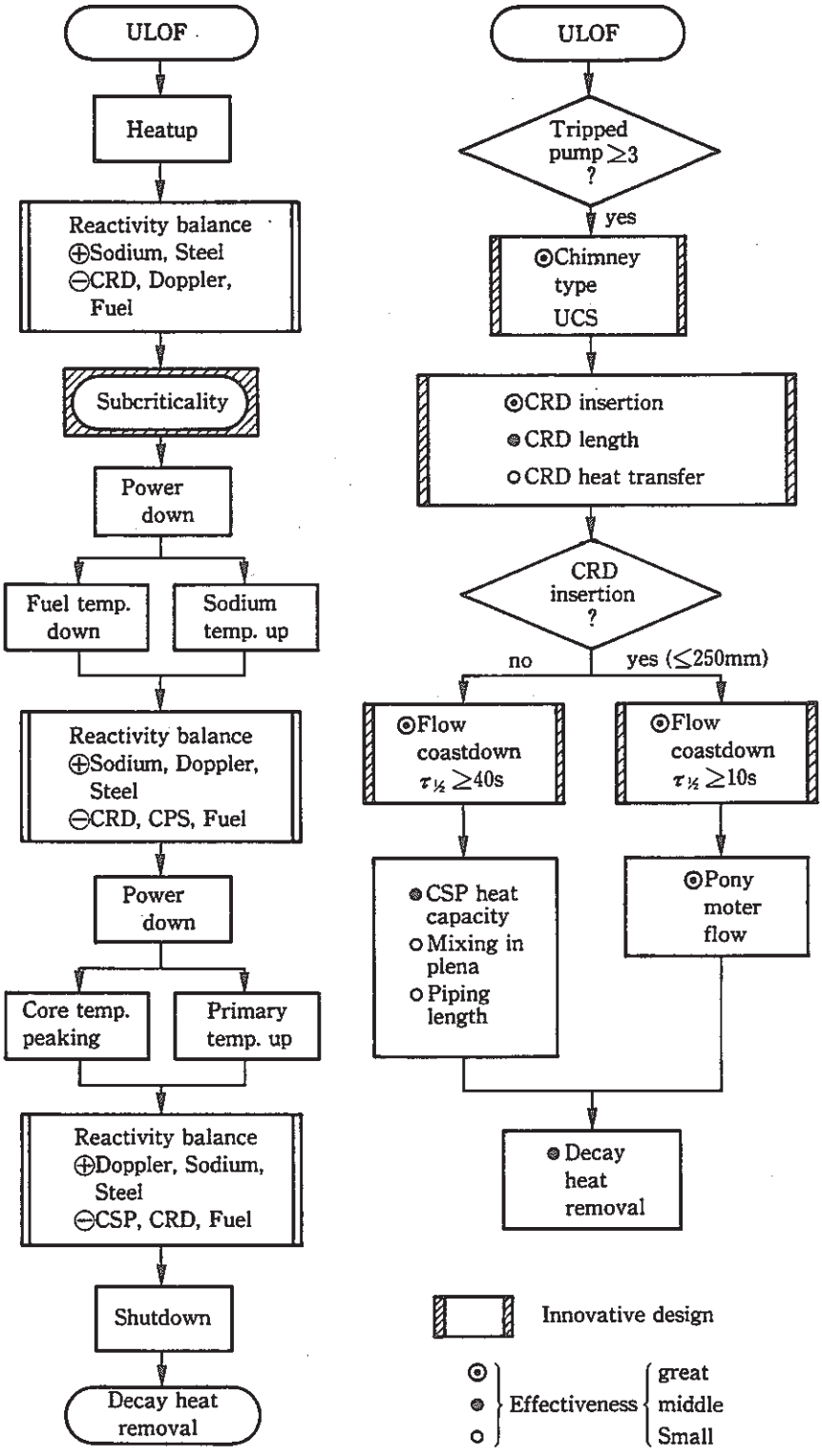

Fig. 7 Successful ULOF scenario and the requirements for attaining the inherently safe plant

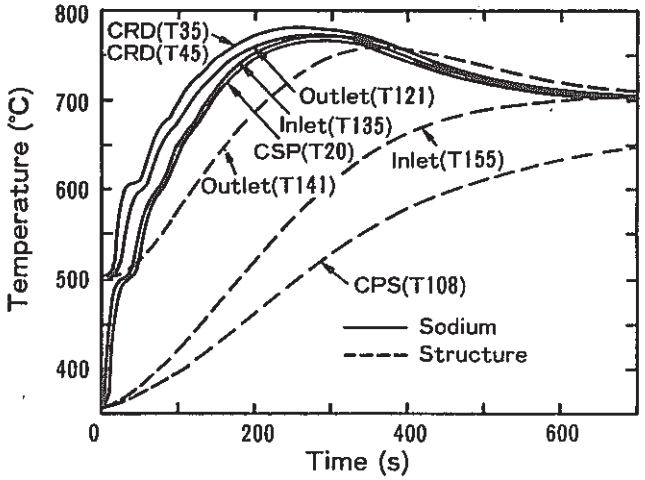

b) Sodium and structure temperatures at the reactor vessel

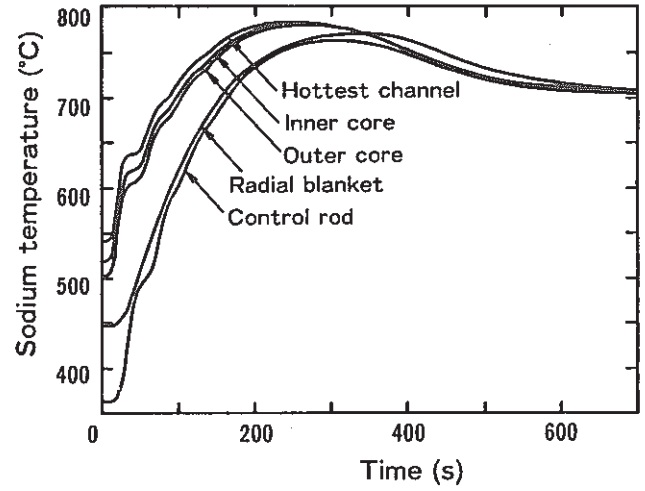

a) Sodium temperatures at the assembly exits

Fig. 8 Predicted ULOHS consequence considering inherent safety features

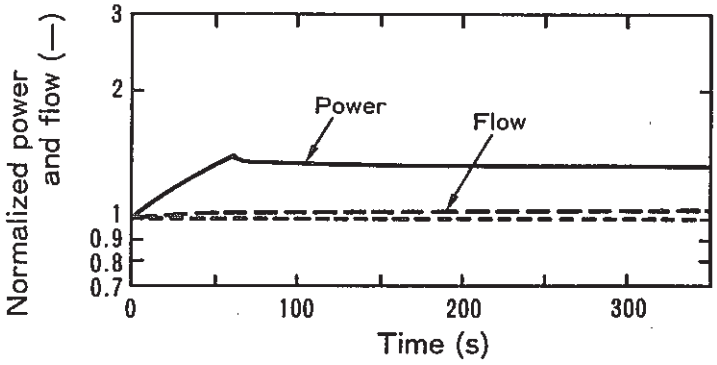

b) Total power and flow

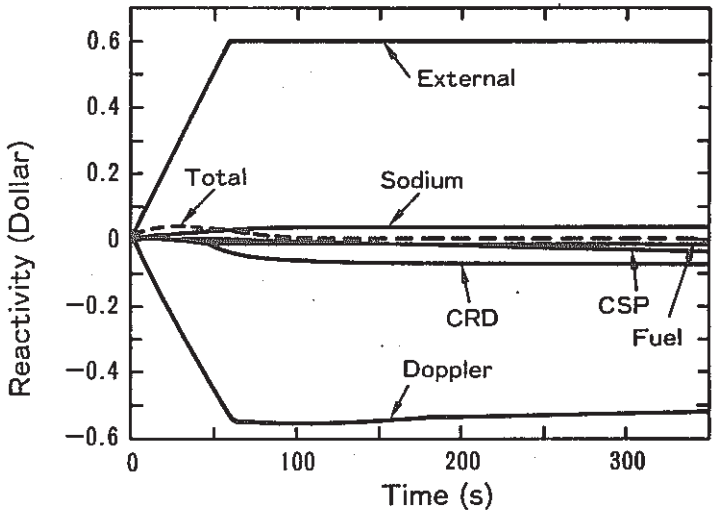

a) Reactivity balance

Fig. 9 Predicted UTOP consequence considering inherent safety features